

Gravitational Waves

I. INTRODUCTION

The wave effects in a lensing system have already been studied in the previous work [1–21]. In these pioneer works, a thin-lens model (e.g. [4]) is usually adopted. Light rays are assumed to be far away from the optic axis and the impact parameter is much larger if compared to the Schwarzschild radius of the lens. The gravity is assumed to be weak. As such, the deflection of light rays caused by the lens is small and light rays are only affected by the lens in regions near the lens. The lens plane, in this case, can be considered “geometrically thin”. The incident and outgoing waves, thus, are on the same lens plane. Outside this lens plane, light rays are assumed to travel in free space. Although this model is successful when explaining the optical images of a lensing system (e.g. [4]), the thin-lens model has some limitations when applied to GWs.

First, by construction the thin-lens model can not be used for light rays near the optic axis. In optical observations, it is feasible to neglect rays the near-axis rays since these rays are sheltered by the lens and can not be observed by a distant observer. However, this might not be the case for GWs. If the wave-length of GWs are comparable to the Schwarzschild radius of the lens, GWs can circle around the lens due to wave effects. In this case, after the scatterer, GWs can continue to travel along the optic axis until arrive at a distant observer. The signals along the optic axis turns out to be an important observational consequence of such a system, which is also an important difference between geometric optics and GWs.

This work aims to address this issue using simulations. We consider the scatterer as a black hole. We aim to simulate GWs passing through the spacetime of a black hole. For these purposes, we assume that GWs are described by linear perturbation theories. In this work, we adopt the Teukolsky equation [22], which is based on the Newman-Penrose (NP) formalism. An advantage of this formalism is that the Weyl tensor Ψ_4 is closely related to GWs at null infinity.

Unlike the conventional $2 + 1$ formalism [23], which is widely used in the literature to solve the Teukolsky equation in the time domain, we focus on the 3D geometry of the wavefront. We present a new method to solve the Teukolsky equation in a $3 + 1$ formalism. We use the finite element method (FEM) rather than the finite difference method (FDM) as usually used in the literature. The FEM is an effective and well-developed method for numerically solving partial differential equations (PDEs). The FEM presents the simulation domain as an assembly

of finite elements. On each finite element, the solution of PDEs is approximated by local shape functions. A continuous PDE problem then can be transformed into a discretized finite element with unknown nodal values. These unknowns form a system of linear algebraic equations. Although this system usually contain a large number of degree of freedoms, the matrices are usually sparse, which can then be solved efficiently using iterative methods, such as the conjugate gradient methods, such as the FDM, which requires regular meshes, the advantage of the FEM is that it can work for complex boundaries so that it can significantly minimize the effects of boundaries.

II. BACKGROUND SPACETIME

We choose the background as Schwarzschild spacetime. We present the line element in terms of the lapse function N and shift vector $\vec{\beta}$

$$ds^2 = g_{\mu\nu} dx^\mu dx^\nu = -N^2 dt^2 + \gamma_{ij} (dx^i + \beta^i dt)(dx^j + \beta^j dt), \quad (2.1)$$

where γ_{ij} is the spatial metric. The Greek letters μ and ν run from 0 to 3 and the Latin indices i and j run from 1 to 3. In isotropic coordinates, the lapse function and γ_{ij} are given by

$$N = \frac{1 - \frac{M}{2\rho}}{1 + \frac{M}{2\rho}}, \quad (2.2)$$

$$\gamma_{ij} = \left(1 + \frac{M}{2\rho}\right)^4 \delta_{ij}, \quad (2.3)$$

where $\rho = \sqrt{x^i x_i}$ is the radius in isotropic coordinates. The shift vector vanishes in this case $\vec{\beta} = (0, 0, 0)$.

The 3+1 Einstein equations with respect to coordinates (t, \vec{x}) are given by

$$\frac{\partial}{\partial t} \gamma_{ij} = -2N K_{ij}, \quad (2.4)$$

$$\frac{\partial}{\partial t} K_{ij} = -D_i D_j N + N(R_{ij} + K K_{ij} - 2K_{il} K^l_j), \quad (2.5)$$

where K_{ij} is the external curvature tensor, R_{ij} is the Ricci tensor for 3D space and D_i is covariant derivative with respect to the 3D spatial metric γ_{ij} . Since γ_{ij} is time independent $\frac{\partial}{\partial t} \gamma_{ij} = 0$, from Eq. (2.4) K_{ij} vanishes on all the hypersurfaces Σ_t

$$K_{ij} = 0. \quad (2.6)$$

In this case, the hypersurface \sum_t is known as the maximal slicing $K = 0$. The lapse functions satisfy the following relations

$$D_i D_j N = N R_{ij} \neq 0, \quad (2.7)$$

$$D_i D^i N = N R = 0. \quad (2.8)$$

In numerical relativity, Eqs. 2.4 and 2.5 constitute a time evolution system as a Cauchy problem. For the background line elements, inserting Eqs. (2.6, 2.7, 2.8) into Eqs. (2.4) and (2.5), the background metrics are consistent with Eqs. (2.4) and (2.5).

In addition to the evolution equations, the 3+1 Einstein's equations are also subject to the Hamiltonian and momentum constraints.

$$R + K^2 - K_{ij} K^{ij} = 0, \quad (2.9)$$

$$D_j K^j_i - D_i K = 0. \quad (2.10)$$

For the background spacetime, the above constraints are automatically satisfied since $R = 0$ and $K = 0$.

III. PERTURBED SPACETIME

A. covariant wave equations

From Eqs. (2.4) and (2.5), the perturbed 3+1 formalism of the Einstein equations are given by

$$\frac{\partial}{\partial t} h_{ij} = -2\delta N K_{ij} - 2N \delta K_{ij}, \quad (3.1)$$

$$\begin{aligned} \frac{\partial}{\partial t} \delta K_{ij} = & -\delta(D_i D_j N) + N \delta R_{ij} + N \delta K K_{ij} \\ & + N K \delta K_{ij} - 2N \delta K_{il} K^l_j - 2N K_{il} \delta K^l_j \\ & + \delta N (R_{ij} + K K_{ij} - 2K_{il} K^l_j). \end{aligned} \quad (3.2)$$

where h_{ij} denotes the perturbed metric

$$h_{ij} = \delta \gamma_{ij}. \quad (3.3)$$

δR_{ij} is the perturbed Ricci tensor, which can be presented in terms of covariant derivatives D and $\delta \Gamma^k_{ij}$

$$\begin{aligned} \delta R_{ij} = & D_k \delta \Gamma^k_{ij} - D_j \delta \Gamma^k_{ik} \\ = & \frac{1}{2} (D^l D_i h_{lj} + D^l D_j h_{il} - D^l D_l h_{ij}) \\ & - \frac{1}{2} D_j D_i (\gamma^{kl} h_{lk}). \end{aligned} \quad (3.4)$$

Although the Christoffel symbol Γ^k_{ij} itself is not a tensor, its perturbation $\delta \Gamma^k_{ij}$ is a tensor, which can be written in a covariant format

$$\delta \Gamma^k_{ij} = \frac{1}{2} \gamma^{kl} (D_i h_{lj} + D_j h_{il} - D_l h_{ij}). \quad (3.5)$$

The perturbation of $2N\delta(D_i D_j N)$ is given by

$$\begin{aligned} 2N\delta(D_i D_j N) = & 2N \left(\frac{\partial^2 \delta N}{\partial x^i \partial x^j} - \Gamma^k_{ij} \partial_k \delta N - \delta \Gamma^k_{ij} \partial_k N \right) \\ = & 2N \left(\frac{\partial^2 \delta N}{\partial x^i \partial x^j} - \Gamma^k_{ij} \partial_k \delta N \right) \\ & - N \partial_k N \gamma^{kl} (D_i h_{lj} + D_j h_{il} - D_l h_{ij}). \end{aligned} \quad (3.6)$$

Unlike non-linear perturbations, Eqs. (3.1) and (3.2) are covariant. To see this point, we consider an infinitesimal coordinate transformation η^i

$$\tilde{\rho}^i = \rho^i + \eta^i. \quad (3.7)$$

For an arbitrary scalar field S and a tensor field T_{ij} , the perturbed quantities transform as

$$\delta \tilde{S} \rightarrow \delta S - \mathcal{L}_{\vec{\eta}} S, \quad (3.8)$$

$$\delta \tilde{T}_{ij} \rightarrow \delta T_{ij} - \mathcal{L}_{\vec{\eta}} T_{ij}, \quad (3.9)$$

where $\mathcal{L}_{\vec{\eta}}$ denotes the Lie derivative. For a scalar field, the Lie derivative gives

$$\mathcal{L}_{\vec{\eta}} S = \eta^k D_k S, \quad (3.10)$$

and for a tensor field, the Lie derivative reads

$$\mathcal{L}_{\vec{\eta}} T_{ij} = T_{ik} D_j \eta^k + T_{kj} D_i \eta^k + \eta^k D_k T_{ij}. \quad (3.11)$$

As such, the perturbed quantities $\delta N, \delta K, h_{ij}$ and δK_{ij} transform as

$$\begin{cases} \delta \tilde{N} \rightarrow \delta N - \eta^k D_k N \\ \delta \tilde{K} \rightarrow \delta K - \eta^k D_k K \\ \tilde{h}_{ij} \rightarrow h_{ij} - \gamma_{ik} D_j \eta^k - \gamma_{kj} D_i \eta^k - \eta^k D_k \gamma_{ij} \\ \delta \tilde{K}_{ij} \rightarrow \delta K_{ij} - K_{ik} D_j \eta^k - K_{kj} D_i \eta^k - \eta^k D_k K_{ij} \end{cases}. \quad (3.12)$$

Inserting the above expressions back into Eqs. (3.1) and (3.2), using Eq. (2.4) and further noting that

$$\begin{aligned} 2N \eta^k D_k K_{ij} = & -2\eta^k D_k N K_{ij}, \\ D_k \gamma_{ij} = & 0, \end{aligned}$$

we can find that Eqs. (3.1) and (3.2) do not change their formats under the infinitesimal coordinate transformation, which means that Eqs. (3.1) and (3.2) are covariant.

Energy conservation $\delta R = 0$

$$\delta(D_i D^i N) = \gamma^{ij} \delta(D_i D_j N) - \gamma^{im} \gamma^{jn} h_{mn} D_i D_j N = 0 \quad (3.13)$$

$$\Gamma_j = D^l h_{lj} \quad (3.14)$$

$$ND^l\Gamma_l = \gamma^{im}\gamma^{jn}h_{mn}R_{ij} = \gamma^{im}\gamma^{jn}h_{mn}\frac{D_iD_jN}{N} \quad (3.15)$$

$$ND^l\Gamma_l = \gamma^{ij}\left(\frac{\partial^2\delta N}{\partial x^i\partial x^j} - \Gamma^k_{ij}\partial_k\delta N\right) - \gamma^{kl}\Gamma_l\partial_k N \quad (3.16)$$

$$D^l\Gamma_l = \frac{1}{\sqrt{|\gamma|}}\frac{\partial}{\partial x_i}\left(\sqrt{|\gamma|}\Gamma_i\right) \quad (3.17)$$

Next, taking the time derivative of Eq. (3.1), and using Eq. (3.2) to eliminate δK_{ij} , we obtain a second order equation for h_{ij}

$$\begin{aligned} \frac{\partial^2}{\partial t^2}h_{ij} = & -2\frac{\partial\delta N}{\partial t}K_{ij} - 2\delta N\frac{\partial K_{ij}}{\partial t} \\ & + 2N\delta(D_iD_jN) - 2N^2\delta R_{ij} \\ & - 2N^2\delta K K_{ij} - 2N^2K\delta K_{ij} + 4N^2\delta K_{il}K^l_j \\ & + 4N^2K_{il}\delta K^l_j - 2N\delta N(R_{ij} + KK_{ij} - 2K_{il}K^l_j). \end{aligned} \quad (3.18)$$

Note that $K_{ij} = 0$, $K = 0$ and $K_i^j = 0$

$$\frac{\partial^2}{\partial t^2}h_{ij} = 2N\delta(D_iD_jN) - 2N^2\delta R_{ij} - 2N\delta N R_{ij}. \quad (3.19)$$

From energy conservation $\delta R = 0$, we have $h = 0$

$$\begin{aligned} \frac{\partial^2}{\partial t^2}h_{ij} = & 2N\left(\frac{\partial^2\delta N}{\partial x^i\partial x^j} - \Gamma^k_{ij}\partial_k\delta N\right) - 2N\delta N R_{ij} \\ & - N^2(D_iD_jh + D^lD_lh_{ij} - D^lD_ih_{lj} - D^lD_jh_{il}) \\ & - N\partial_k N\gamma^{kl}(D_ih_{lj} + D_jh_{il} - D_lh_{ij}). \end{aligned} \quad (3.20)$$

Using the identity

$$D^lD_ih_{lj} = D_iD^lh_{lj} + R^m_{ji}{}^nh_{mn} + R_i^lh_{lj}, \quad (3.21)$$

we obtain

$$\begin{aligned} \frac{\partial^2}{\partial t^2}h_{ij} = & 2N\left(\frac{\partial^2\delta N}{\partial x^i\partial x^j} - \Gamma^k_{ij}\partial_k\delta N\right) - 2N\delta N R_{ij} \\ & + N^2D^lD_lh_{ij} - N^2(D_i\Gamma_j + D_j\Gamma_i) \\ & - N^2(2R^m_{ij}{}^nh_{mn} + R_i^lh_{lj} + R_j^lh_{li}) \\ & - N\partial_k N\gamma^{kl}(D_ih_{lj} + D_jh_{il} - D_lh_{ij}). \end{aligned} \quad (3.22)$$

The above equation is consistent with Eq.(34) in the literature, if γ_{ij} is flat space. However, in our case, the curvature terms do not vanish since the background γ_{ij} is not flat.

For numerical reasons, it is more convenient to write the covariant derivatives D^lD_l in Eq. (3.22) in terms of ordinary partial derivatives

$$N^2D^lD_lh_{ij} = c^2\nabla^2h_{ij} - \frac{32(2\rho - M)^2\rho^3M}{(2\rho + M)^7}\frac{\rho^l}{\rho}\partial_lh_{ij}, \quad (3.23)$$

where $\nabla^2 = \partial_i\partial^i$ and the coefficient c^2 is defined by

$$c^2 = \frac{16\rho^4(2\rho - M)^2}{(2\rho + M)^6}. \quad (3.24)$$

The last term on the RHS in Eq. (3.22) can also be simplified as

$$\begin{aligned} & N\partial_k N\gamma^{kl}(D_ih_{lj} + D_jh_{il} - D_lh_{ij}) \\ & = f_\Gamma\frac{\rho^l}{\rho}[\partial_ih_{lj} + \partial_jh_{il} - \partial_lh_{ij} - 2\Gamma^m_{ij}h_{lm}], \end{aligned} \quad (3.25)$$

where

$$f_\Gamma = \frac{64(2\rho - M)M\rho^4}{(2\rho + M)^7}. \quad (3.26)$$

We rewrite the Ricci tensor in the second term on the RHS in Eq. (3.22) as

$$N^2\gamma^{lk}R_{ik}h_{lj} = f_R\delta^{lk}\tilde{R}_{ik}h_{lj}, \quad (3.27)$$

where R_{ij} and \tilde{R}_{ij} are given by

$$\begin{aligned} R_{ij} &= \frac{4M}{\rho^3(2\rho + M)^2}(\delta_{ij}\rho^2 - 3\rho_i\rho_j) \\ &= \frac{4M}{\rho^3(2\rho + M)^2}\tilde{R}_{ij}, \end{aligned} \quad (3.28)$$

$$\tilde{R}_{ij} = \delta_{ij}\rho^2 - 3\rho_i\rho_j. \quad (3.29)$$

The coefficient f_R is defined by

$$f_R = \frac{64(2\rho - M)^2M\rho}{(2\rho + M)^8}. \quad (3.30)$$

The terms associated with the Riemann tensor can be written as

$$\begin{aligned} N^2R^m_{ij}{}^nh_{mn} &= N^2\gamma^{mp}\gamma^{nq}R_{pijq}h_{mn} \\ &= f_R\delta^{mp}\delta^{nq}\tilde{R}_{pijq}h_{mn}, \end{aligned} \quad (3.31)$$

where

$$R_{pijq} = \frac{M(2\rho + M)^2}{4\rho^7}\tilde{R}_{pijq}, \quad (3.32)$$

$$\tilde{R}_{ijij} = 2\rho^2 - 3\rho_i^2 - 3\rho_j^2, \quad (i \neq j) \quad (3.33)$$

$$\tilde{R}_{ijik} = -3\rho_j\rho_k, \quad (i \neq j \neq k). \quad (3.34)$$

Combining all the above expressions, we obtain

$$\begin{aligned} \frac{\partial^2}{\partial t^2}h_{ij} = & 2N\left(\frac{\partial^2\delta N}{\partial x^i\partial x^j} - \Gamma^k_{ij}\partial_k\delta N\right) - \frac{8M(2\rho - M)}{\rho^3(2\rho + M)^3}\delta N\tilde{R}_{ij} \\ & - N^2(\partial_i\Gamma_j + \partial_j\Gamma_i - 2\Gamma^k_{ij}\Gamma_k) \\ & + c^2\nabla^2h_{ij} + f_\rho\frac{\rho^k}{\rho}\partial_kh_{ij} - 2f_R\delta^{mp}\delta^{nq}\tilde{R}_{pijq}h_{mn} \\ & - f_R(\delta^{lk}\tilde{R}_{ik}h_{lj} + \delta^{lk}\tilde{R}_{jk}h_{li}) \\ & - f_\Gamma\frac{\rho^l}{\rho}(\partial_ih_{lj} + \partial_jh_{il} - 2\Gamma^m_{ij}h_{lm}), \end{aligned} \quad (3.35)$$

where

$$f_\rho = \frac{32(2\rho - M)\rho^3 M^2}{(2\rho + M)^7}. \quad (3.36)$$

The above equation is the core equation we aim to solve this work, which governs the evolution of GWs in Schwarzschild spacetime. The momentum constraints give

$$\sum_{i=1}^3 \left(\partial_i - \frac{2M(4\rho - M)}{\rho^2(4\rho^2 - M^2)} x^i \right) h_{ij} = 0 \quad (3.37)$$

$$\Gamma_j = \frac{(2\rho)^4}{(2\rho + M)^4} \frac{4M}{4\rho^2 - M^2} \frac{x^i}{\rho} h_{ij} \quad (3.38)$$

$$\begin{cases} \tilde{\partial}_0 \zeta_1 = \tilde{\partial}_1 h_+ + \tilde{\partial}_2 h_- \\ \tilde{\partial}_0 \zeta_0 + \tilde{\partial}_2 \zeta_2 = -\tilde{\partial}_1 \zeta_1 \\ \tilde{\partial}_2 \zeta_0 - \tilde{\partial}_0 \zeta_2 = \tilde{\partial}_1 h_- - \tilde{\partial}_2 h_+ \end{cases}.$$

where

$$\tilde{\partial}_i = \partial_i - \frac{2M(4\rho - M)}{\rho^2(4\rho^2 - M^2)} x^i \quad (3.39)$$

$$\begin{cases} h_+ = h_{11} \\ h_- = h_{12} = h_{21} \\ \zeta_0 = h_{00} \\ \zeta_1 = h_{01} = h_{10} \\ \zeta_2 = h_{02} = h_{20} \\ h_{22} = -\zeta_0 - h_+ \end{cases}.$$

B. isotropic wave speed

The parameter c in Eq. (3.35) represents the speed of GWs measured by a static observer $(\frac{\partial}{\partial t})^a$ at spatial infinity. Unlike the conventional wave equation, a notable feature of Eq. (3.35) is that the wave speed varies with respect to different places in space.

Figure 1 shows c as a function of ρ/M . As expected, the speed of wave c goes back to the speed of light in vacuum $c \sim 1$ if the place is distant from the center of the black hole

$$\lim_{\rho/M \rightarrow \infty} c = 1. \quad (3.40)$$

However, when the place is close to the black hole, c becomes much smaller. At horizon the speed of wave completely becomes zero

$$\lim_{\rho \rightarrow M/2} c = 0. \quad (3.41)$$

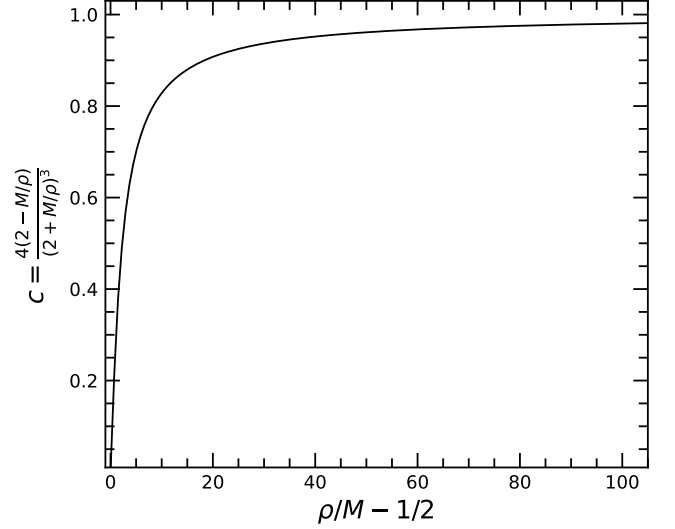


FIG. 1. The speed of wave c as a function of ρ/M . We choose the horizontal axis as $\rho/M - 1/2$ for convenience. When observers are far away from the black hole or the mass of the black hole tends to zero, c goes back to the speed of light in vacuum. On the contrary, at horizon $\rho/M \rightarrow 1/2$, the speed of wave becomes zero.

As we shall show later, this varying speed of wave c plays an important role in the propagation of GWs in curved spacetime.

Moreover, it is important to note that c also equals to the speed of light rays in curved space time. From the line element of Eq. (2.1), for a null curve $ds^2 = 0$ (not necessarily null geodesics), we obtain

$$0 = -N^2 dt^2 + \left(1 + \frac{M}{2\rho}\right)^4 dx^2, \quad (3.42)$$

which gives

$$\frac{dx^2}{dt^2} = \frac{N^2}{\left(1 + \frac{M}{2\rho}\right)^4} = \frac{16\rho^4(2\rho - M)^2}{(2\rho + M)^6} = c^2. \quad (3.43)$$

This demonstrates that GWs in Schwarzschild spacetime travel at the same speed as those of light rays. It is also worth noting that c is isotropic. The speed of wave does not depend on the directions of its propagation.

C. perturbed constraints

In addition to the wave equation, the perturbation of constraint Eq. (2.9) gives

$$\delta R + 2K\delta K - \delta K_{ij}K^{ij} - K_{ij}\delta K^{ij} = 0, \quad (3.44)$$

which simply implies that

$$\delta R = 0. \quad (3.45)$$

Taking the trace of Eq. (3.1), we obtain

$$\delta K = 0. \quad (3.46)$$

The perturbation of constraint Eq. (2.10) reduces to

$$D^j \delta K_{ji} = 0. \quad (3.47)$$

The constraints should be satisfied simultaneously along with the evolution equation of GWs.

IV. THE INITIAL CONDITIONS

We assume that the incident waves are far away from the black hole. In this case, GWs can be considered as traveling in vacuum. In the limit $M \rightarrow 0$, Eqs. (3.1, 3.2, 3.18) reduce to

$$\frac{\partial}{\partial t} h_{ij}^T = -2\delta K_{ij}, \quad (4.1)$$

$$\frac{\partial}{\partial t} \delta K_{ij} = \delta R_{ij}, \quad (4.2)$$

$$\frac{\partial^2}{\partial t^2} h_{ij}^T = -2\delta R_{ij}. \quad (4.3)$$

From Eq. (3.4), the perturbed Ricci tensor becomes

$$\delta R_{ij} = -\frac{1}{2} \nabla^2 h_{ij}^T. \quad (4.4)$$

Equation (4.3) then becomes

$$\frac{\partial^2}{\partial t^2} h_{ij}^T = \nabla^2 h_{ij}^T. \quad (4.5)$$

The above equation can also be obtained from Eq. (3.35) by noting that $f_\rho \rightarrow 0, f_R \rightarrow 0, f_\Gamma \rightarrow 0, c^2 \rightarrow 1$ when $M \rightarrow 0$.

Equation (4.5) has analytical solutions

$$h_{ij}^T(t, \vec{\rho}) = H_{ij} \cos(\omega t - k^i \rho_i), \quad (4.6)$$

where \vec{k} is the wave vector, $\vec{\rho}$ is the position vector and ω is the angular frequency. H_{ij} is a constant tensor field. The Dirac gauge conditions $\nabla^i h_{ij}^T = 0$ gives

$$k^i H_{ij} = 0. \quad (4.7)$$

If we choose the incident wave along the x -axis, the above condition means that H_{ij} is transverse and does not have x components

$$H_{xi} = 0, \quad (4.8)$$

Moreover, as h_{ij} is trace-less from Eq. (4.9) we obtain

$$\delta R_i^i = -\frac{1}{2} \nabla^2 h_i^i{}^T = 0. \quad (4.9)$$

Given the Dirac gauge condition, we also have

$$\nabla^i \delta K_{ij} = -\frac{1}{2} \frac{\partial}{\partial t} \nabla^i h_{ij}^T = 0. \quad (4.10)$$

As such, Eq. (4.6) satisfies the perturbed constraints of Eqs. (2.9, 2.10). **If the initial condition satisfies the equation of constraints, the following evolution should obey the constraints as well.**

V. FINITE ELEMENT METHOD

To numerically solve Eq. (3.18), we use the finite element method. Unlike the conventional methods such as, the finite difference method, the FEM is based on the *weak formulation* (or *variational formulation*) of the PDEs. Therefore we will first introduce the *weak formulation* of the wave equations, which can be obtained by multiplying Eq. (3.35) with a test function Ψ and then integrate over a domain Ω . For convenience, we adopt the following notion

$$\langle f, g \rangle = \int_{\Omega} f(x)^* g(x) dx. \quad (5.1)$$

Equation (3.18) can be presented as

$$\begin{aligned} & \langle \Psi, \frac{\partial^2}{\partial t^2} h_{ij}^T e^i \otimes e^j \rangle \\ &= \langle \Psi, (c^2 \nabla^2 h_{ij}^T + f_\rho \partial_\rho h_{ij}^T) e^i \otimes e^j \rangle \\ & - \langle \Psi, (f_R \delta^{mp} \tilde{R}_{im} h_{pj}^T + f_R \delta^{mp} \tilde{R}_{jp} h_{mi}^T) e^i \otimes e^j \rangle \\ & - 2 \langle \Psi, f_R \delta^{mp} \delta^{nq} \tilde{R}_{pijq} h_{mn}^T e^i \otimes e^j \rangle \\ & - \langle \Psi, f_\Gamma \frac{\rho^p}{\rho} (\partial_i h_{pj}^T + \partial_j h_{ip}^T - 2\Gamma_{ij}^m h_{pm}^T) e^i \otimes e^j \rangle, \end{aligned} \quad (5.2)$$

where $e^i \otimes e^j$ is the tensor basis. In the free evolution scheme, the trace-less tensor h_{ij}^T has 5 DoFs, which should be evolved simultaneously. We denote the basis of these 5 components as ϵ^α , which is related to $e^i \otimes e^j$ by

$$e^i \otimes e^j = C_{ij}^{\alpha} \epsilon^\alpha. \quad (5.3)$$

Given such a basis, the tensor field $h_{ij}^T e^i \otimes e^j$ can be presented in terms of ϵ^σ

$$h_{ij}^T e^i \otimes e^j = H_\sigma \epsilon^\sigma. \quad (5.4)$$

The coefficient H_σ is related to h_{ij}^T by

$$h_{ij}^T = C_{ij}^{\sigma} H_\sigma, \quad (5.5)$$

where $C_{ij}^{\sigma} C_{ij}^{\alpha} = \delta^{\sigma\alpha}$.

The *test* function Ψ for a vector field can be constructed in the form

$$\Psi = \phi \otimes \epsilon^\alpha, \quad (5.6)$$

where ϕ is chosen in such a way that it vanishes on the subset of boundaries with Dirichlet boundary conditions $\partial\Omega_D$

$$\mathcal{V} := \{\phi : \phi \in H^1(\Omega), \phi|_{\partial\Omega_D} = 0\}. \quad (5.7)$$

$H^1(\Omega) = W^{1,2}(\Omega)$ is called the first order *Sobolev space* meaning that ϕ and its first order weak derivatives $\partial_x \phi$ are square integrable

$$\|\phi\|_{H^1(\Omega)} = \left[\int_{\Omega} \sum_{|\alpha| \leq 1} |\partial_x^\alpha \phi(x)|^2 dx \right]^{\frac{1}{2}} < \infty.$$

If h_{ij}^T in Eq. (5.2) holds for any test function Ψ , h_{ij}^T is called the *weak solution* and Eq. (5.2) is called the *weak formulation*.

A. spatial discretization

In the Finite Elements Methods (FEM), the domain Ω is decomposed into subdomains Ω_i , which consist of rectangles or triangles. This is called *decomposition* or *triangulation*. The vertices of rectangles and triangles in the domain Ω are called mesh points or nodes. Let Ω_h denote the set of all nodes of the decomposition. On each node, we construct a scalar test function $\phi_i \in V$, $i = 1, \dots, N$, where V is the space defined in Eq. (5.7) and N is the total number of nodes in the domain. The scalar test function ϕ_i is required to have the property

$$\phi_i(p^k) = \delta_{ik}, \quad i, k = 1, \dots, N, \quad p^k \in \Omega_h.$$

As such, ϕ_i has non-zero values only on the node with $k = i$ and its adjacent subdomains, which is called the influential zones. However, it vanishes on other parts of the domain Ω . The test function ϕ_i constructed this way is called the *scalar shape function*. Clearly, $\phi_i \in V$ on different nodes are linearly independent. We denote the space spanned by ϕ_i as $V_h := \text{span}\{\phi_i\}_{i=1}^N$, which is a subspace of V . The vector shape functions can be constructed from the scalar shape functions with ϕ_i for each component of the vector field

$$\Psi_{l,\tau} = \phi_l \otimes \epsilon^\tau, \quad (5.8)$$

where ϵ^τ is the basis of a vector.

Given the shape function, the tensor fields $h_{ij}^T e^i \otimes e^j$ can be expanded as

$$h_{ij}^T e^i \otimes e^j = H_\sigma \epsilon^\sigma = H_\sigma^k \phi_k \otimes \epsilon^\sigma, \quad (5.9)$$

where the component H_σ is a scalar field that can be further expanded by $H_\alpha = H_\alpha^k \phi_k$.

Since Eq. (5.2) holds for any test functions Ψ , we can choose Ψ as shape functions over all different nodes in the domain. The left-hand-side of Eq. (5.2) reads,

$$\begin{aligned} \langle \phi_l \otimes \epsilon^\tau, \frac{\partial^2}{\partial t^2} h_{ij}^T e^i \otimes e^j \rangle &= \langle \phi_l \otimes \epsilon^\tau, \phi_k \otimes \epsilon^\sigma \rangle \frac{\partial^2}{\partial t^2} H_\sigma^k \\ &= \langle \phi_l, \phi_k \rangle \otimes \delta_\tau^\sigma \frac{\partial^2}{\partial t^2} H_\sigma^k, \end{aligned} \quad (5.10)$$

where the index l runs over $1, \dots, N$ and τ runs over $1, \dots, 5$. Similarly, for the first term on the right-hand-side of Eq. (5.2), we obtain

$$\begin{aligned} \langle \phi_l \otimes \epsilon^\tau, c^2 \nabla^2 h_{ij}^T e^i \otimes e^j \rangle &= \langle \phi_l \otimes \epsilon^\tau, c^2 \nabla^2 \phi_k \otimes \epsilon^\sigma \rangle H_\sigma^k \\ &= - \langle (\nabla c^2) \phi_l, \nabla \phi_k \rangle \otimes \delta_\tau^\sigma H_\sigma^k - \langle c^2 \nabla \phi_l, \nabla \phi_k \rangle \otimes \delta_\tau^\sigma H_\sigma^k \\ &\quad + \langle \phi_l, c^2 \hat{n} \cdot \nabla H_\sigma \rangle_{\partial\Omega} \otimes \delta_\tau^\sigma \end{aligned} \quad (5.11)$$

where for the last term, we have used integration by parts. $\langle \phi_l, c^2 \hat{n} \cdot \nabla H_\sigma \rangle_{\partial\Omega} \otimes \delta_\tau^\sigma$ represents the integration over boundaries of the simulation domain $\partial\Omega$. This term is related to the boundary conditions in FEM, for which we shall discuss in detail in the next few sections.

For other terms, we have

$$\begin{aligned} \langle \phi_l \otimes \epsilon^\tau, f_\rho \frac{\rho^m}{\rho} \partial_m h_{ij}^T e^i \otimes e^j \rangle \\ = \langle \phi_l \otimes \epsilon^\tau, f_\rho \frac{\rho^m}{\rho} \partial_m \phi_k \otimes \epsilon^\sigma \rangle H_\sigma^k \end{aligned} \quad (5.12)$$

$$\begin{aligned} &= \langle \phi_l, f_\rho \partial_\rho \phi_k \rangle \otimes \delta_\tau^\sigma H_\sigma^k, \\ \langle \phi_l \otimes \epsilon^\tau, f_R \delta^{mp} \tilde{R}_{ip} h_{mj}^T e^i \otimes e^j \rangle \\ &= \langle \phi_l \otimes \epsilon^\tau, f_R \delta^{mp} \tilde{R}_{ip} C_{mj}^\sigma C^{ij}_\alpha \phi_k \otimes \epsilon^\alpha \rangle H_\sigma^k \\ &= \langle \phi_l, f_R \delta^{mp} \tilde{R}_{ip} C_{mj}^\sigma C^{ij}_\alpha \phi_k \rangle \otimes \delta_\tau^\alpha H_\sigma^k, \end{aligned} \quad (5.13)$$

$$\begin{aligned} \langle \phi_l \otimes \epsilon^\tau, f_R \delta^{mp} \delta^{nq} \tilde{R}_{pijq} h_{mn}^T e^i \otimes e^j \rangle \\ = \langle \phi_l \otimes \epsilon^\tau, f_R \delta^{mp} \delta^{nq} \tilde{R}_{pijq} C_{mn}^\sigma C^{ij}_\alpha \phi_k \otimes \epsilon^\alpha \rangle H_\sigma^k \end{aligned} \quad (5.14)$$

$$\begin{aligned} &= \langle \phi_l, f_R \delta^{mp} \delta^{nq} \tilde{R}_{pijq} C_{mn}^\sigma C^{ij}_\alpha \phi_k \rangle \otimes \delta_\tau^\alpha H_\sigma^k, \\ \langle \phi_l \otimes \epsilon^\tau, f_\Gamma \frac{\rho^p}{\rho} \partial_i h_{pj}^T e^i \otimes e^j \rangle \\ &= \langle \phi_l \otimes \epsilon^\tau, f_\Gamma \frac{\rho^p}{\rho} C_{pj}^\sigma C^{ij}_\alpha \partial_i \phi_k \otimes \epsilon^\alpha \rangle H_\sigma^k \\ &= \langle \phi_l, f_\Gamma \frac{\rho^p}{\rho} \partial_i \phi_k C_{pj}^\sigma C^{ij}_\alpha \rangle \otimes \delta_\tau^\alpha H_\sigma^k, \end{aligned} \quad (5.15)$$

$$\begin{aligned} \langle \phi_l \otimes \epsilon^\tau, f_\Gamma \frac{\rho^p}{\rho} \Gamma_{ij}^m h_{pm}^T e^i \otimes e^j \rangle \\ = \langle \phi_l \otimes \epsilon^\tau, f_\Gamma \frac{\rho^p}{\rho} \Gamma_{ij}^m C_{pm}^\sigma C^{ij}_\alpha \phi_k \otimes \epsilon^\alpha \rangle H_\sigma^k \\ = \langle \phi_l, f_\Gamma \frac{\rho^p}{\rho} \Gamma_{ij}^m C_{pm}^\sigma C^{ij}_\alpha \phi_k \rangle \otimes \delta_\tau^\alpha H_\sigma^k. \end{aligned} \quad (5.16)$$

Inserting the above expressions back into Eq. (5.2), we obtain $5 \times N$ different equations, which form a linear

system. It is more convient to present Eq. (5.2) in a matrix format

$$\begin{cases} M \frac{\partial}{\partial t} V = -M^B \frac{\partial}{\partial t} H - FH, \\ \frac{\partial}{\partial t} H = V, \end{cases} \quad (5.17)$$

where F is defined by

$$F = A + D^c - D^\rho + 2D^{\text{Ricci}} + 2D^{\text{Riemann}} + 2D^{\Gamma_1} - 2D^{\Gamma_2}. \quad (5.18)$$

The elements of matrices are defined by

$$\begin{cases} M_{(lk) \otimes (\tau\sigma)} = \langle \phi_l, \phi_k \rangle \otimes \delta_\tau^\sigma \\ M_{(lk) \otimes (\tau\sigma)}^B = \langle c\phi_l, \phi_k \rangle_{\partial\Omega} \otimes \delta_\tau^\sigma \\ D_{(lk) \otimes (\tau\sigma)}^c = \langle \nabla(c^2)\phi_l, \nabla\phi_k \rangle \otimes \delta_\tau^\sigma \\ A_{(lk) \otimes (\tau\sigma)} = \langle c^2\nabla\phi_l, \nabla\phi_k \rangle \otimes \delta_\tau^\sigma \\ D_{(lk) \otimes (\tau\sigma)}^\rho = \langle \phi_l, f_\rho \frac{\rho^m}{\rho} \partial_m \phi_k \rangle \otimes \delta_\tau^\sigma \\ D_{(lk) \otimes (\tau\sigma)}^{\Gamma_1} = \langle \phi_l, f_\Gamma \frac{\rho^p}{\rho} \partial_i \phi_k C_{pj}^\sigma C^{ij}_\alpha \rangle \otimes \delta_\tau^\alpha \\ D_{(lk) \otimes (\tau\sigma)}^{\Gamma_2} = \langle \phi_l, f_\Gamma \frac{\rho^p}{\rho} \Gamma_{ij}^m C_{pm}^\sigma C^{ij}_\alpha \phi_k \rangle \otimes \delta_\tau^\alpha \\ D_{(lk) \otimes (\tau\sigma)}^{\text{Ricci}} = \langle \phi_l, f_R \delta^{mp} \tilde{R}_{ip} C_{mj}^\sigma C^{ij}_\alpha \phi_k \rangle \otimes \delta_\tau^\alpha \\ D_{(lk) \otimes (\tau\sigma)}^{\text{Riemann}} = \langle \phi_l, f_R \delta^{mp} \delta^{nq} \tilde{R}_{pijq} C_{mn}^\sigma C^{ij}_\alpha \phi_k \rangle \otimes \delta_\tau^\alpha \end{cases} \quad (5.19)$$

B. time discretization

For the time discretization, we use the following scheme.

$$M \frac{V^n - V^{n-1}}{k} = -M^B \frac{H^n - H^{n-1}}{k} - F[\theta H^n + (1-\theta)H^{n-1}], \quad (5.20)$$

$$\frac{H^n - H^{n-1}}{k} = \theta V^n + (1-\theta)V^{n-1}. \quad (5.21)$$

The superscript n indicates the number of a time step and $k = t_n - t_{n-1}$ is the length of the present time step. Using Eq. (5.20) to eliminate H^n in Eq. (5.21) and Eq. (5.21) to eliminate V^n in Eq. (5.20), we can present H^n and V^n in terms of V^{n-1} and H^{n-1}

$$\begin{aligned} & [M + k\theta M^B + k^2\theta^2 F]H^n \\ & = [M + k\theta M^B - k^2\theta(1-\theta)F]H^{n-1} + kMV^{n-1}, \end{aligned} \quad (5.22)$$

$$\begin{aligned} & [M + k\theta M^B + k^2\theta^2 F]V^n \\ & = [M - k(1-\theta)M^B - k^2\theta(1-\theta)F]V^{n-1} - kFH^{n-1}. \end{aligned} \quad (5.23)$$

Given the knowledge of V^{n-1} and H^{n-1} at a previous time step, we can solve H^n and V^n from the above two linear equations.

When $\theta = 0$, the scheme is called the forward or explicit Euler method. If $\theta = 1$, it reduces to the backward or implicit Euler method. The scheme adopted in this work is called the *Crank-Nicolson Scheme*, namely $\theta = 1/2$, which uses the midpoint between two different time steps. This scheme is *implicit* and is of second-order accuracy. An advantage of the *implicit* method is that it can be stable for arbitrary step sizes if the scheme is *upwind* (see. Chapter 2 in Ref. [24]). However, a stable scheme does not guarantee a correct solution to the wave equation. We need to resolve the waveforms as well. For this purpose, in our simulations, we set $k = \lambda/10$ and the size of the mesh $\sigma < \lambda/15$, where λ is the wave length.

VI. LINEAR SOLVERS

The numbers of independent equations in Eqs. (5.22) and (5.23) are called the degree-of-freedom (DOF) of the system. In FEM, the DOF is usually very large, which can be easily up to 10^9 . Therefore, direct methods such as the LU decomposition are inefficient in this case. One has to use the iterative methods. However, it is important to note that, matrices D^c , D^ρ , D^{Γ_1} , D^{Γ_2} , D^{Ricci} , D^{Riemann} are not symmetric in our case. Some conventional methods such as the Conjugate Gradient (CG) method can not be used here. Instead, we use the GMRES method [25], which does not require any specific properties of the matrices.

VII. BOUNDARY CONDITIONS

For test functions $\phi \in \mathcal{V}$, the Dirichlet boundary conditions do not appear explicitly in Eqs. (5.22) and (5.23), which are called *essential boundary conditions*. However, the Neumann conditions have to appear explicitly in the formulation, which is called *natural boundary conditions*. The boundary conditions only appear in these terms associated with the Laplacian operator ∇^2 , namely, the last term in Eq. (5.11)

$$\begin{aligned} & \langle \phi_l, c^2 \hat{n} \cdot \nabla H_\sigma \rangle_{\partial\Omega} \otimes \delta_\tau^\sigma \\ & = \langle \phi_l, c^2 \hat{n} \cdot \nabla H_\sigma \rangle_{\partial\Omega_1} \otimes \delta_\tau^\sigma + \langle \phi_l, c^2 \hat{n} \cdot \nabla H_\sigma \rangle_{\partial\Omega_2} \otimes \delta_\tau^\sigma, \end{aligned} \quad (7.1)$$

where $\partial\Omega_1$ represents the boundaries of the simulation domain and $\partial\Omega_2$ represents the horization of black hole.

On $\partial\Omega_1$ we impose the absorbing boundary condition

$$\langle \phi_l, c^2 \hat{n} \cdot \nabla H_\sigma \rangle_{\partial\Omega_1} \otimes \delta_\tau^\sigma = -\langle c\phi_l, \phi_k \rangle_{\partial\Omega_1} \otimes \delta_\tau^\sigma \frac{\partial}{\partial t} H_\sigma^k, \quad (7.2)$$

where we have used

$$\hat{n} \cdot \nabla H_\sigma = -\frac{1}{c} \frac{\partial H_\sigma}{\partial t} \quad \text{on} \quad \partial\Omega_1 \times (0, T]. \quad (7.3)$$

The absorbing boundary condition is also called the *non-reflecting boundary* conditions or *radiation boundary* condition. These boundary conditions can eliminate the reflections of waves on boundaries, which enables us to simulate the propagation of waves in free space using a finite simulation domain.

At horizon $\partial\Omega_2$, we have

$$\lim_{\rho \rightarrow M/2} c^2 = 0. \quad (7.4)$$

A notable feature of our formulation is that the boundary term on $\partial\Omega_2$ vanishes

$$\langle \phi_l, c^2 \hat{n} \cdot \nabla H_\sigma \rangle_{\partial\Omega_2} \otimes \delta_\tau^\sigma = 0. \quad (7.5)$$

As such, our formalism can naturally avoid the singularity at horizon and does not involve artificial boundary conditions at horizon.

VIII. SIMULATION SETUPS

We choose the simulation domain as a cylinder with a radius of R_{cylinder} and length of L_{cylinder} . We assume

that the source of GWs is far away from the simulation domain and the incident waves travel along the axis of the cylinder (x -axis). Unlike a cube domain which is usually adopted in simulations, a cylinder domain can minimize the effect of boundaries on waveforms since in our simulations the waveform is a function of azimuth. Moreover, we choose the length of the cylinder L_{cylinder} long enough so that the wavefront of the incident wave is not distorted by the black hole at the surface of the simulations domain. The incident GWs at $x = -L_{\text{cylinder}}/2$ can be well approximated by plane waves and is normal to the x -axis. The wave vector \vec{k} of the incident GWs at $x = -L_{\text{cylinder}}/2$ can be considered as a constant.

IX. NULL GEODESIC

$$\begin{cases} \frac{d^2\mu'}{d\phi^2} = \frac{3M-r}{\rho^2} \frac{d\rho}{dr} \\ \frac{d\rho}{dr} = \frac{1}{2} \left(1 + \frac{r-M}{\sqrt{r^2-2Mr}} \right) \end{cases}. \quad (9.1)$$

-
- [1] S. Deguchi and W. D. Watson, Phys. Rev. D **34**, 1708 (1986).
 - [2] A. K. Meena and J. S. Bagla, (2019), arXiv:1903.11809 [astro-ph.CO].
 - [3] S. Deguchi and W. D. Watson, Astrophys. J. **307**, 30 (1986).
 - [4] P. Schneider, J. Ehlers, and E. E. Falco, *Gravitational Lenses* (Springer, 1992).
 - [5] A. A. Ruffa, The Astrophysical Journal **517**, L31 (1999).
 - [6] F. De Paolis, G. Ingrosso, A. A. Nucita, and A. Qadir, *Conference on Astronomical Telescopes and Instrumentation Waikoloa, Hawaii, August 22-28, 2002*, Astron. Astrophys. **394**, 749 (2002), arXiv:astro-ph/0209149 [astro-ph].
 - [7] R. Takahashi and T. Nakamura, Astrophys. J. **595**, 1039 (2003), arXiv:astro-ph/0305055 [astro-ph].
 - [8] T. T. Nakamura and S. Deguchi, Progress of Theoretical Physics Supplement **133**, 137 (1999).
 - [9] T. Suyama, R. Takahashi, and S. Michikoshi, Phys. Rev. **D72**, 043001 (2005), arXiv:astro-ph/0505023 [astro-ph].
 - [10] P. Christian, S. Vitale, and A. Loeb, Phys. Rev. **D98**, 103022 (2018), arXiv:1802.02586 [astro-ph.HE].
 - [11] D. J. D’Orazio and R. Di Stefano, (2019), arXiv:1906.11149 [astro-ph.HE].
 - [12] A. F. Zakharov and Y. V. Baryshev, Classical and Quantum Gravity **19**, 1361 (2002).
 - [13] L. Dai and T. Venumadhav, (2017), arXiv:1702.04724 [gr-qc].
 - [14] K. Liao, M. Biesiada, and X.-L. Fan, Astrophys. J. **875**, 139 (2019), arXiv:1903.06612 [gr-qc].
 - [15] D. L. Jow, S. Foreman, U.-L. Pen, and W. Zhu, (2020), arXiv:2002.01570 [astro-ph.HE].
 - [16] J.-P. Macquart, Astron. Astrophys. **422**, 761 (2004), arXiv:astro-ph/0402661.
 - [17] T. T. Nakamura, Phys. Rev. Lett. **80**, 1138 (1998).
 - [18] L. Dai, S.-S. Li, B. Zackay, S. Mao, and Y. Lu, Phys. Rev. D **98**, 104029 (2018), arXiv:1810.00003 [gr-qc].
 - [19] Z. Cao, L.-F. Li, and Y. Wang, Phys. Rev. D **90**, 062003 (2014).
 - [20] C.-M. Yoo, T. Harada, and N. Tsukamoto, Phys. Rev. D **87**, 084045 (2013), arXiv:1302.7170 [gr-qc].

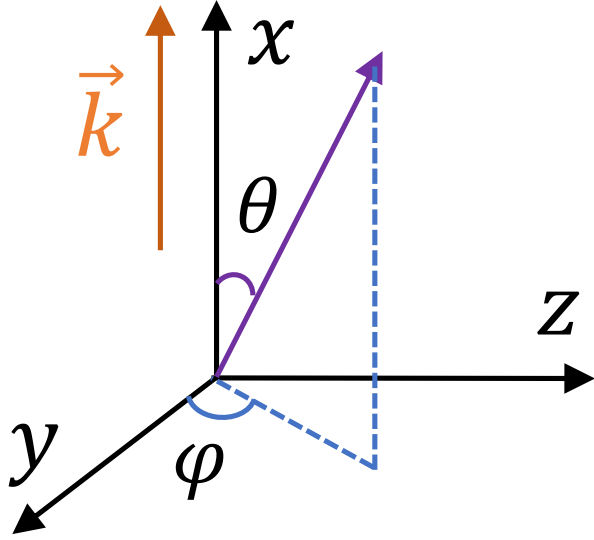


FIG. 2. The coordinate system of our simulations. The wave vector \vec{k} of the incident wave is parallel to the x -axis. The wavefront of the incident wave is normal to the x -axis.

The triangulation of simulation domain

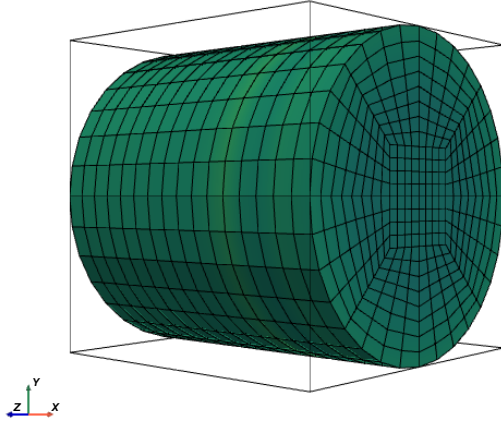


FIG. 3. The triangulation of our simulation domain. We only show the refinement of 2^5 for illustrative purposes. The incident waves travel along the x -axis from $x = -\infty$ to $x = +\infty$. The wavefront of the incident wave at $x = -L_{\text{cylinder}}/2$ is normal to the x -axis.

- [21] Y. Nambu, S. Noda, and Y. Sakai, Phys. Rev. D **100**, 064037 (2019), arXiv:1905.01793 [gr-qc].
- [22] S. A. Teukolsky, Astrophys. J. **185**, 635 (1973).
- [23] W. Krivan, P. Laguna, P. Papadopoulos, and N. Anderson, Phys. Rev. D **56**, 3395 (1997), arXiv:gr-qc/9702048.
- [24] C. Grossmann, H.-G. Roos, and M. Stynes, *Numerical treatment of partial differential equations*, Vol. 154 (Springer, 2007).
- [25] D. M. Young and J. Y. Chen, (1996), 10.2172/409863.